J Mater Sci (2009) 44:5662–5672
DOI 10.1007/s10853-009-3798-8

Preparation and characterization of composite materials obtained by pressure infiltration of aluminum in sintered SiC/kaolin preforms

N. Freitas · S. A. Pianaro · S. M. Tebcherani · F. N. Nadal · E. A. T. Berg

Received: 19 January 2009 / Accepted: 5 August 2009 / Published online: 15 August 2009

Abstract The present work involved the preparation and characterization of SiC–Al composites containing kaolin concentrations varying from 10 to 50% in substitution of the major SiC phase. Ceramic preforms were produced, controlling the granulometric fraction of SiC/kaolin. After sintering at 1100 °C, these preforms were highly porous. XRD analyses revealed the existence of quartz and SiC phase. During the infiltration process, the molten aluminum reacted preferentially with the quartz and with other aluminosilicates in the preforms, reducing them and precipitating alumina and silica in the microstructure, which also showed excess aluminum that did not react in the process. The silica and silicates of the preform, by reacting preferentially with the aluminum, preventing the formation of Al_4C_3 phase. The SiC–kaolin–Al composites developed here can be used in applications that require high flexural strength (240–300 MPa), low density, and surface hardness of 180–380 kgf/mm^2.

Introduction

Composites are materials that have distinct chemical and/or physical phases distributed within a continuous phase called the matrix [1]. CMCs (ceramic matrix composites) are the most recent materials in the field of composites. The correct choice of the matrix and the reinforcement, from the standpoint of their processing and chemical composition, is extremely important to ensure their good performance. However, another major factor that directly affects performance is the presence of an interfacial region at the ceramic/metal junction, which is of fundamental importance for the material's final properties [2].

Ceramic/metal composites have potential applications in the aerospace and automotive industries and in a variety of other structural applications, due to the combination of physical and mechanical properties of metals and ceramics. They combine the physical properties of metals, such as high ductility and toughness, with the properties of high modulus and strength of ceramics. These advanced materials offer an advantageous alternative for high performance in aeronautical engineering design, considering their low strength-to-weight ratio in the fabrication of components [3].

Due to its high technological potential for the manufacture of composites, silicon carbide has been exhaustively studied as a matrix in aluminum infiltration processes by squeeze-casting. The properties of this type of composite are strongly dependent on a variety of factors such as mean particle size and particle size distribution, particle shape, the properties of the molten metal (surface tension, viscosity), wettability of the particles by the molten metal (liquid–solid interface), atmosphere, height of the perform, and the volumetric percentage of SiC that is part of the matrix [4–7]. On the one hand, long infiltration periods and small particle sizes affect the composite's rupture modulus positively, while on the other, the presence of Si coating the SiC particles impair this property, reducing the material's mechanical strength. Under optimal conditions of infiltration, composites can be obtained with 300 MPa of mechanical strength and a porosity of less than 3% [4].

N. Freitas · S. A. Pianaro (✉) · S. M. Tebcherani · F. N. Nadal · E. A. T. Berg
Laboratório Interdisciplinar de Materiais Cerâmicos—LIMAC, Departamento de Engenharia de Materiais, Universidade Estadual de Ponta Grossa, Av. Carlos Cavalcanti, 4748, Ponta Grossa 84030-900, PR, Brazil
e-mail: sap@uepg.br

By varying the infiltration pressure and temperature of an aluminum alloy containing 10% of Si and 1.2% of Mg in Al_2O_3/SiC preforms, composites can be obtained ranging in mechanical strength from 70 to 558 MPa and with densities varying from 1.78 to 2.78 g/cm^3 [8].

Low density composites (1.99 g/cm^3) with values of mechanical strength between 380 and 441 MPa can be obtained by the infiltration of Al–SiC powders through polymer. During the pyrolysis of the polymer, the active aluminum reactions with the carbon and nitrogen atmospheres present, forming AlN and Al_4Si_3 phases as well as Al_4C_3 phase [9]. The infiltration of pure silicon carbide with aluminum is normally characterized by the presence of Al_4C_3 phase in the microstructure, which is hygroscopic, impairing the properties of the composite [10, 11].

Chemical processes can also be used [12]. Ceramic foam composed of Al_2O_3/SiC can be obtained from an aqueous solution composed of aluminum sulfate, ammonium sulfate, and silicon carbide powder. Under thermal treatment, SiC particles are deposited upon Al_2O_3 particles, resulting in a highly porous preform with a homogeneous distribution of pores and SiC and Al_2O_3 particles. Maximum values of mechanical strength of 271 MPa were characterized in that work.

Studies on the effect of processing variables of composites obtained from a particulate SiC_p-6061 system infiltrated with Al [13] revealed that rapid cooling in water improved the properties of bending strength and hardness of the composite when compared with the composites cooled at the normal rate in the furnace. Moreover, the reduction in SiC particle size from 85 to 14 μm increased the values of mechanical strength and hardness. Heat treatments close to the eutectic temperature also favored composites with greater strength. It was also found that the use of silica helped increase the mechanical strength.

A study of another particulate system, based on the Al–SiC_p–Mg system [14], indicated that Mg produces the formation of Mg_2Si precipitates in the matrix, reducing the porosity of the composite. Furthermore, the presence of Mg was found to prevent the appearance of the deleterious Al_4C_3 phase and to increase the hardness.

Composites with mechanical strength greater than 500 MPa were obtained from SiC preforms coated with polymethylsiloxane (PMS) processed by spray-dryer and infiltrated with aluminum by squeeze-casting [15].

The single phase of $Al_{85}Y_8Ni_5Co_2$ glass-reinforced Al-based MMCs with high strength combined with considerable ductility have been produced by powder metallurgy methods. The maximum stress increases from 155 MPa for pure Al to 255 and 295 MPa for composites with 30 and 50 vol.% of glassy phase, respectively [16].

Kaolin is a raw material mostly used as silica and alumina source in traditional ceramics compositions, not being studied until the present time as additive in the preparation of SiC–Al composites obtained by suqeeze-casting. In such a way, the aim of the present work is to prepare composites materials by pressure infiltration of aluminum in sintered SiC/kaolin preforms, to evaluate its effect in the inhibition of the Al_4C_3 deleterious phase and to characterize the physical, mechanical, and microstructural properties of the composites as function of the kaolin concentration in the composition.

Experimental

The raw materials used in this work were Silicon Carbide (Saint-Gobain green crystal LG F-90), Campo Alegre Kaolin, and Aluminum–Silicon alloy (ALCOA AlSi 11-838).

Preparation and characterization of the raw materials

The silicon carbide (SiC), with a particle size of 125 μm, was dry-milled in a ball mill and separated into different granulometric fractions using GRANUTEST ABNT 200, 325, and 400 μm mesh sieves. This procedure resulted in three particle size distributions, i.e., those that passed through the 200 μm mesh and retained in the 325 mesh (called #200), those that passed through the 325 mesh and were retained in the 400 mesh (called #325) and those that passed through the 400 μm mesh (called #400). Part of the fine particles (#400) were wet-milled for 3 h in a high speed mill (BP ENGENHARIA) to obtain silicon carbide with a mean particle size of about 10 μm. A fraction of these particles was added to the composition to increase the mechanical strength of the green test specimens.

Previous test specimen compaction studies conducted in our laboratory using the #200 fraction with the addition of the fine fraction resulted in better workability of green bodies with high porosity, so this fraction was chosen to formulate the compositions of the present work.

The composition of the Campo Alegre kaolin contains a fraction of coarser quartz particles in addition to the colloidal quartz also present. To reduce the size of this fraction, the raw material was milled until no residue was left in the 400 μm mesh sieve.

The aluminum–silicon alloy was cut into smaller pieces suitable for melting in a crucible.

The raw material powders and the mixtures were characterized by particle size distribution using a CILAS 920 granulometer. For the mineral identification, the raw materials were analyzed by X-ray diffraction using a SHIMADZU XRD-6000 diffractometer.

Composition, preparation, and characterization of the ceramic preforms

The compositions of the preforms (Table 1) were prepared with mixtures, in mass percent, of SiC and kaolin fine particles with silicon carbide #200. These compositions were defined up to a limit of 50% of kaolin. A SiC–Al composition without added kaolin was prepared in order to compare its physical and mechanical properties against those of the composites containing kaolin. This system was structurally analyzed, which demonstrated the formation of the Al_4C_3 phase in the pure SiC–Al composite, corroborating other studies [9–11].

Having defined the compositions, the raw materials were weighed on a digital balance (MARTE AS-5500), mixed and homogenized with the addition of 10% water to confer plasticity on the conformational process. The compositions were then sifted through a 0.5 mm mesh nylon sieve and stored in plastic bags for later conformation.

The test specimens were prepared in a stainless steel mold with internal dimensions of 13 × 60 mm^2, under a pressure of 65 kgf/cm^2 in a 15 ton hydraulic press (SCHULZ PHS). After high-pressure conformation, the test specimens were oven dried (110 °C/4 h) and sintered in an electric furnace (EDGCON 5P-3000) at 1100 °C for 3 h.

The sintered porous preforms were characterized following the methodology proposed by Pérsio Souza Santos [17]. The following ceramic assays were carried out: linear retraction, water absorption, apparent density, apparent porosity, and flexural strength.

Infiltration of the ceramic preforms and characterization of the composites

The infiltration process was carried out using a squeeze-casting equipment. The sintered preformed were initially preheated in an electric muffler (EDGCON 3P-7000). At the same time, the aluminum was melted and held at 850 °C, at which temperature the slag was removed from the molten metal.

The pressure infiltration chamber was cleaned and lubricated with MOLYKOTE G paste and graphite powder, and then preheated between 250 and 300 °C. The ceramic preforms were quickly transferred to the infiltration chamber and the molten aluminum poured over them. A pressure of 70 MPa was then applied to the set using a hydraulic piston, enabling the infiltration of the aluminum into the pores of the preform. Lastly, excess aluminum was removed from the surface of the composites. After this procedure, the infiltrated test specimens were again placed in the furnace to remove excess surface aluminum. After cooling, the surfaces of the composites were finished by polishing with a SiC grinding wheel (CARBORUNDUM).

The densities of the composites were determined by the Archimedes method. The flexural strength of the test specimens was determined using a SHIMADZU AG-I 10 kN universal testing machine. Samples of the composite were subjected to a Vickers hardness test using a SHIMADZU HMV-2 micro-hardness meter. The hardness data were collected from random regions of the composite. The analysis involved the application of a 2 kg load for 30 s. The results obtained corresponded to an average of five points for each composition.

The microstructural analysis was carried out by scanning electron microscopy (SEM, SHIMADZU SS-550). To this end, the samples were cut with a precision sectioning saw (BUEHLER IsoMet low speed saw) using QUIMAT-IC-II cutting fluid. After embedding the samples in polyester resin, they were sandpapered with 150, 320, 400, and 600 grit SiC emery paper (NORTON) and polished in alumina suspensions of 1.0 and 0.3 μm in an AROTEC APL-4 polishing machine. Finally, their surfaces were ultrasound cleaned to remove polishing residues and then oven dried.

The phases were determined by X-ray diffraction using a SHIMADZU XRD-6000 diffractometer. The preform compositions in powder form were calcined at 1100 °C in an electric muffler, after which they were milled until 100% of the material passed through the 325 μm mesh sieve and then analyzed. The infiltrated test specimens were milled and analyzed by the same procedure.

Table 1 Preform compositions

Raw materials	Compositions (mass %)				
	C10	C20	C30	C40	C50
SiC #200	80	70	60	50	40
SiC fine particles	10	10	10	10	10
Kaolin	10	20	30	40	50

Results and discussion

Granulometric characterization of the compositions

Figure 1 shows the granulometric distribution curves corresponding to the SiC 200, SiC 300, and SiC 400 powders with the addition of 10% of SiC fine particles. The distribution was not homogeneous due to the presence of the SiC fine particles, characterized on the curve by presenting 100% of the particles with sizes below 30 μm. The curves corresponding only to the coarser fractions displayed a

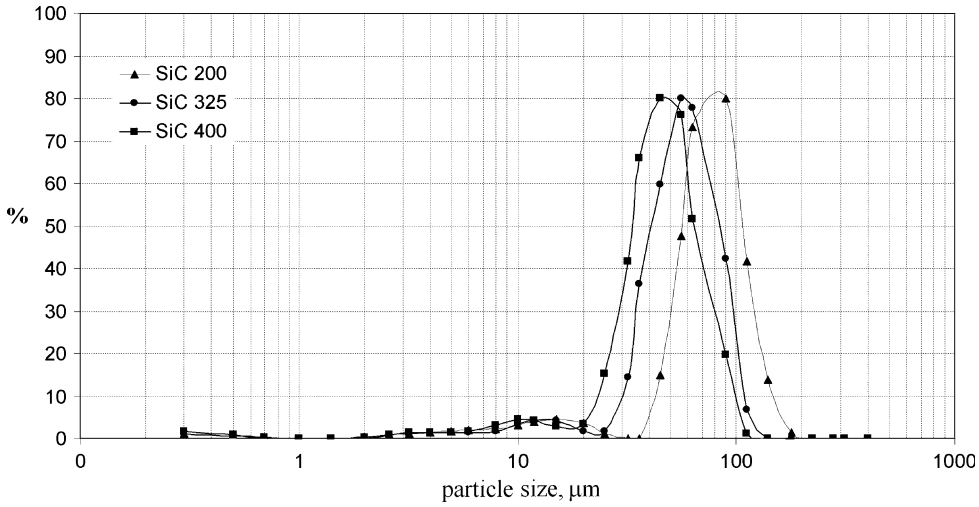

Fig. 1 Particle size distribution curves of SiC 200, SiC 325, and SiC 400

homogeneous distribution with mean d_{50} particle sizes of 70, 50, and 40 μm, respectively, for the SiC 200, SiC 325, and SiC 400 fractions.

In our previous studies, we found that, for the current experimental conditions, the best results were attained with test specimens composed of the SiC 200 granulometric fraction, since there was complete infiltration of the preforms. The complete infiltration of preforms composed of finer particle size distributions required increasing the infiltration pressure and temperature, which hampered the process. Therefore, in the present study, the optimized condition adopted for the formation of the matrix was a composition consisting of SiC #200 + 10% fine particles, preheating of the preform to 250 °C, aluminum melt temperature of 850 °C, and infiltration pressure of 70 MPa.

The graphs in Fig. 2 show the granulometric distribution corresponding to the different amounts of kaolin added to the SiC matrix, as indicated by the compositions listed in Table 1. The addition of kaolin led to a fairly wide particle distribution, whose concentration varied as a function of the added kaolin, resulting in a highly heterogeneous final distribution of particle sizes. Obviously, the distribution with the highest concentration of fine particles corresponds to composition C50. As can be seen, 100% of the particles of the kaolin raw material presented a diameter of less than 60 μm, with the coarser fraction of this distribution attributed to the quartz particles present as impurities in the raw material.

Physical characterization of the ceramic preforms

Table 2 lists the properties of water absorption, apparent porosity, apparent density, and flexural strength of the sintered ceramic preforms corresponding to the three granulometric fractions of SiC, i.e., #200, #325, and #400, plus the C10 to C50 compositions listed in Table 1.

The apparent porosity of the SiC systems increased as the particle size of the matrix decreased, resulting in greater water absorption and a reduction of apparent density, which varied from 1.71 g/cm^3 for the SiC #200 to 1.53 g/cm^3 for the SiC #400. The mechanical strength of the preforms containing kaolin was far greater than that of the preform composed solely of SiC plus 10% of fine particles, greatly facilitating the handling of the performs for infiltration. The addition of just 10% of kaolin to the SiC #200 sufficed to double its mechanical strength, which reached a maximum value of 1.64 MPa in the C30 composition. Additions of more than 30% kaolin inverted this trend, with a drop in mechanical strength, which showed 1.23 and 1.0 MPa in the C40 and C50 compositions, respectively. From these results, it can be concluded that kaolin additions of more than 30% not only reduce the apparent density but also cause the larger SiC particles to act as matrix reinforcement, rendering the preforms more brittle.

Figure 3 shows the microstructures of the preforms sintered with different concentrations of kaolin, comparing them to the sintered preform of SiC #200 plus 10% fine SiC particles. Note that, as the kaolin concentration increases, the larger pores are filled and the SiC particles are almost completely coated with kaolin particles (composition C50). With kaolin contents exceeding 20%, the action of the temperature causes the large pores of the SiC matrix to become obstructed, increasing the apparent density. With kaolin contents of 30% or more, the amount of kaolin is sufficiently large, competing with the SiC matrix and forming a highly porous refractory coatings but with small pore sizes. This coating envelops the SiC grains and the porosity again increases, reducing the apparent density of 1.90 g/cm^3 (C20) to 1.63 g/cm^3 (C50).

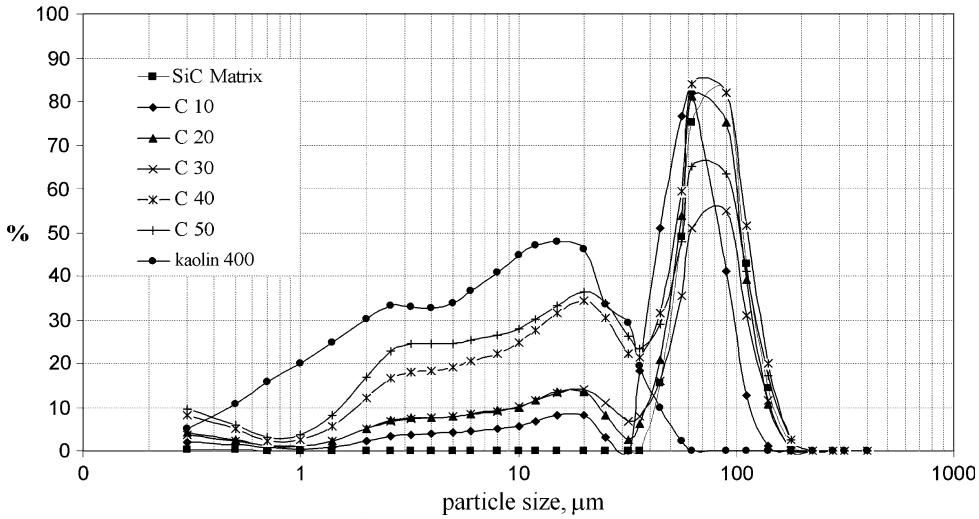

Fig. 2 Particle size distribution curves for the composition of the SiC matrix without and with the addition of different amounts of kaolin and of the kaolin raw material

Table 2 Physical properties of the SiC and SiC/kaolin preforms

Composition	Water absorption (%)	Apparent porosity (%)	Apparent density (g/cm^3)	Flexural strength (MPa)
SiC #200	27.71	46.27	1.71	0.66
SiC #325	31.30	49.53	1.62	–
SiC #400	34.63	51.40	1.53	–
C10	22.01	39.00	1.81	1.22
C20	19.50	36.22	1.90	1.53
C30	20.61	37.46	1.81	1.64
C40	24.33	41.28	1.72	1.23
C50	27.05	43.70	1.63	1.00

Ceramic phases and microstructures

The XRD results of the C10 and C50 compositions before sintering showed the following ceramic phases: silicon carbide, SiC (Moissanite—5/ITH), aluminum silicate hydrate, $Al_2Si_2O_5(OH)_4$ (kaolinite), and silicon oxide, SiO_2 (quartz). This highly crystalline quartz is present as an impurity in the Campo Alegre kaolin. A fraction of this mineral is presented in the form of extremely fine particles of a colloidal nature. Figure 4 shows the XRD spectra of the powders of compositions C10–C50 calcined at 1100 °C.

These spectra showed only peaks corresponding to the SiC phases (Moissanite—5/ITH) and SiO_2 (Quartz), but, according to the literature [17], an endothermic reaction occurs at around 500 °C, which is due to the dehydration or decomposition of kaolin, forming the target kaolin phase of $2Al_2O_3{\cdot}4SiO_2$ composition. At 925 °C, the target kaolin layers condense, forming the spinel phase of $2Al_2O_3{\cdot}3SiO_2$ composition through the disappearance of 1 mol of SiO_2 from the structure. As the temperature increases, an exothermic reaction occurs between 950 and 1100 °C, and the spinel structure transforms into mullite with an approximate composition of $3Al_2O_3{\cdot}2SiO_2$, releasing one additional mol of SiO_2. Thus, considering that the heat treatment temperature to obtain the preforms was 1100 °C, besides the SiC and SiO_2 phases characterized by XRD, other aluminosilicates were probably present, constituting the ceramic preforms, which were not identified by XRD due to the superimposition of other phases. It was also found that as the kaolin content in the composition increased, the quartz peaks increased in intensity while the SiC peaks diminished.

Figure 5 shows the XRD diffractograms of the C10–C50 infiltrated preforms, which showed the following ceramic phases: silicon carbide, SiC—"Moissanite—5/ITH"; Alumina (Al_2O_3); metallic silicon (Si); and metallic aluminum (Al).

A comparison against the diffractograms of the sintered preforms revealed a drastic phase transformation resulting from the infiltration with metallic aluminum. The quartz reacted strongly in the infiltration process. The presence of metallic silicon suggests that the quartz was reduced in the process by the molten aluminum, which can be confirmed by the identification of alumina in the XRD diffractograms

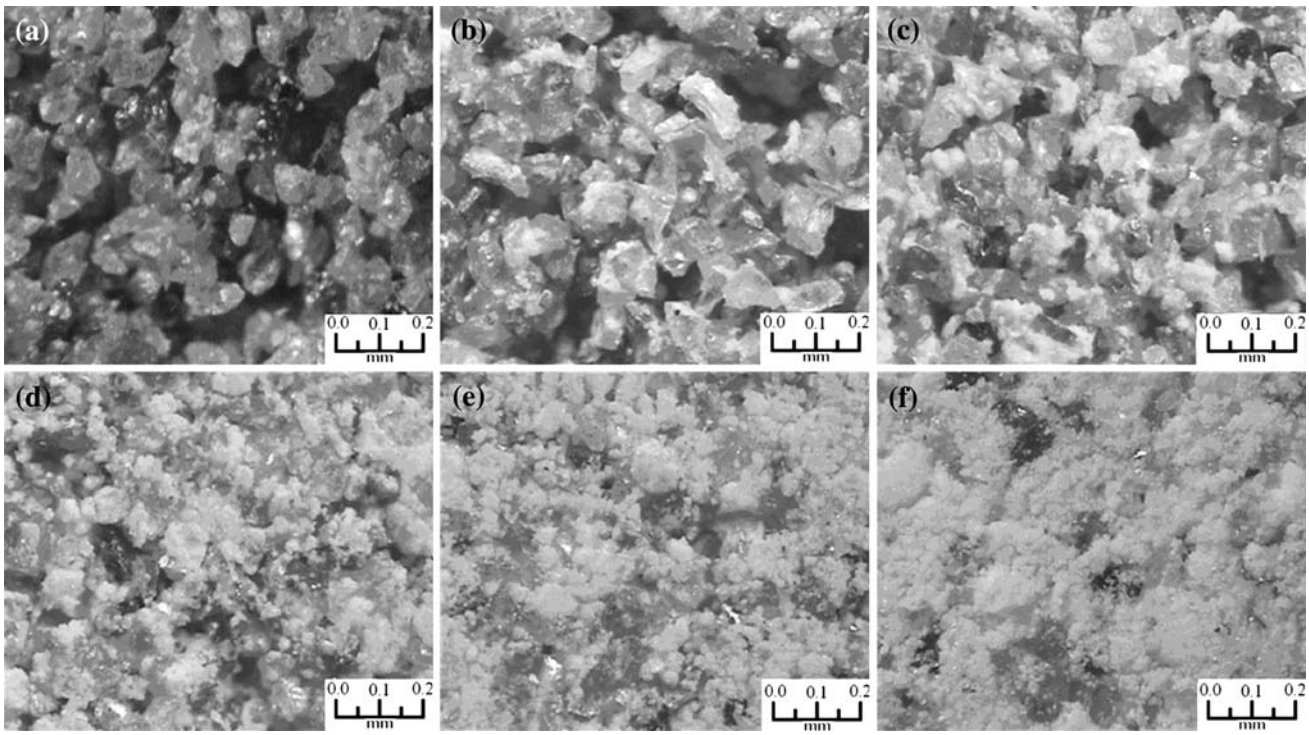

Fig. 3 Microstructures of the preforms: **a** SiC 200, **b** C10, **c** C20, **d** C30, **e** C40, and **f** C50

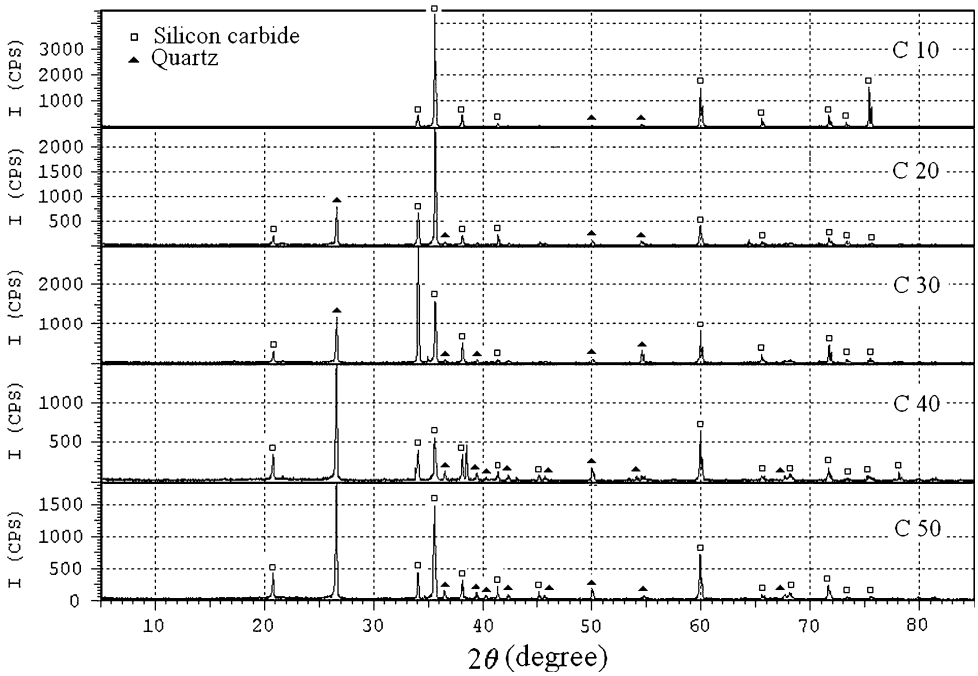

Fig. 4 X-ray diffractograms of the calcined preforms containing different concentrations of kaolin in their composition

and the disappearance of the peaks corresponding to quartz. The excess aluminum, which did not react with the quartz of the preform, remained as metallic aluminum. In the diffractograms, also note that with increasing kaolin content in the composition, a greater quantity of alumina was formed from the reduction of the quartz, since the latter was present as an impurity in the kaolin.

The reduction of silica and formation of alumina follows the reaction mechanism [18] shown below:

$$3SiO_{2(s)} + 4Al_{(l)} \Leftrightarrow 2Al_2O_{3(s)} + 3Si_{(s)} \quad (1)$$

where s is the connotation that designates solid and l designates liquid. The product α–Al_2O_3 is initially formed on the surface of the SiO_2 particles (interface between the

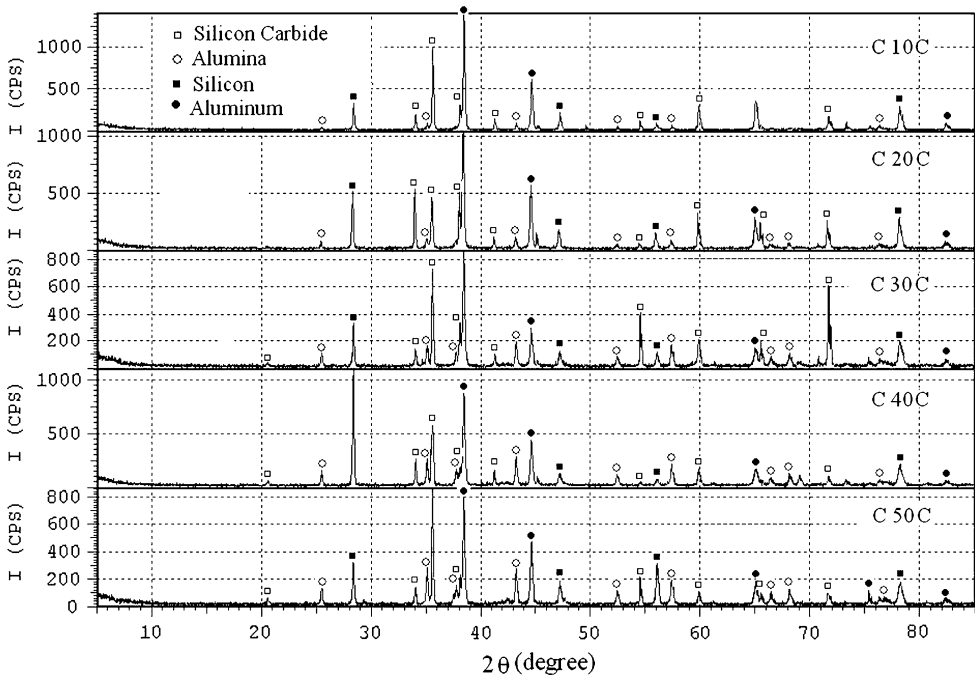

Fig. 5 X-ray diffractograms of the of the C10C to C50C composites

preform and the molten aluminum) and subsequently the reaction takes place inside the quartz particles [18]. The SiC remained unaltered, i.e., it did not react with the metallic aluminum during the infiltration. However, studies have shown that the infiltration of pure SiC with aluminum can generate the Al_4C_3 phase [9–11], according to the following reaction:

$$4Al_{(l)} + 3SiC_{(s)} \Leftrightarrow Al_4C_{3(s)} + 3Si_{(s)} \quad (2)$$

The presence of this phase is deleterious, resulting in the degradation of the composite, since it is unstable and reacts slowly with air humidity, forming aluminum hydroxide [11], according to the reaction:

$$Al_4C_{3(s)} + 12H_2O_{(l)} \Leftrightarrow 3CH_{4(s)} + 4Al(OH)_{3(s)} \quad (3)$$

Another potential product of formation is the Al_4SiC_4 phase [19]. This phase is also deleterious to the composite's properties. In the present study, none of these phases was characterized. This finding may be explained by the preferential reaction of the liquid aluminum with the quartz and other aluminosilicates at high temperatures. Thus, the corrosion of the SiC grains and the formation of Al_4C_3 phase is avoided, in which the presence of humidity leads to the degradation reaction presented in 3. It can therefore be concluded that the presence of quartz, like that of other aluminosilicates, is essential to the formation of SiC/Al composites that are stable with respect to humidity-related degradation. In a recent paper, a novel MMC casting technique was introduced using a foam pattern of the PPS/SiC_p/CMC. It results in a more uniform distribution of SiC particles then the other casting technique, reducing the contact time between SiC and matrix avoiding the formation of Al_4C_3 deleterious phase [20]. Considering the probable existence of mullite in the ceramic preforms, an example of the reaction of this phase with liquid aluminum [21] occurs as follows:

$$(8 + x)Al + 3Al_6Si_2O_{13} \Rightarrow 13Al_2O_3 + 6Si + xAl \quad (4)$$

A comparison of the microstructures of the SiC 200–Al composite and the SiC 200 + kaolin–Al composites containing different concentrations of kaolin is shown in Fig. 6. The considerable granulometric difference between SiC (d_{50} = 70 μm) and kaolin (d_{50} = 15 μm) led to wide microstructural variability, as evidenced with increasing amounts of kaolin in the composition, which showed an increasingly "fine" microstructure. Comparing these micrographs against those of Fig. 3, i.e., with their respective preforms, it is clear that the aluminum exerted a strongly reactive power over the highly porous surface aggregates of the preforms, resulting in highly densified microstructures.

To verify the distribution of the chemical elements in the matrix of the composites and to find a correlation between the phase distribution in the microstructure, a mapping study of the elements was carried out by EDX in the microstructures of the composites characterized by SEM. These analyses involved the composites whose initial composition contained 10% (C10) and 50% (C50) of kaolin, i.e., minimum and maximum amounts of the mineral additive. The results of these analyses are presented in Figs. 7 and 8, respectively. The C10 composition consisted of coarse angular SiC grains with a mean size of 70 μm,

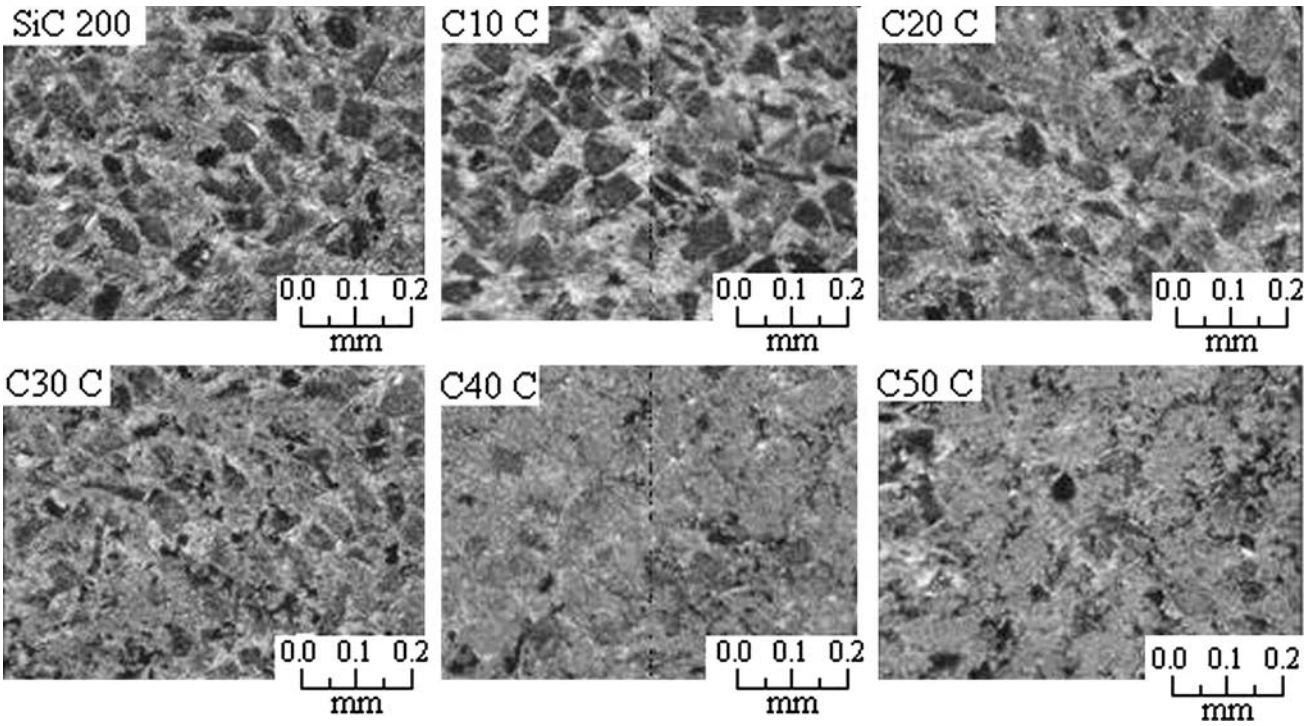

Fig. 6 Optic microscopy image of the SiC–Al composites without and with different kaolin concentrations

which are clearly visible because they contrast easily in the microstructure since they display a darker shade. Most of the silicon characterized by EDX corresponded to the silicon of the SiC phase. The metallic silicon, also present and a product of reaction 1, was located preferentially close to the SiC phase in the microstructure. Aluminum may appear in the metallic form (brighter) or combined with oxygen, forming alumina, which is also a product of the reaction presented in 1 or 4, if one considers the existence of mullite in the preform. Proof of this is that the oxygen-rich regions in the microstructure are always accompanied by the element aluminum, suggesting the formation of alumina, with the presence also of metallic aluminum (brighter).

Figure 8 presents the analysis of the elements corresponding to the C50C composite. A comparison of the microstructures of the C50C and C10C composites reveals a significant difference. Due to the lower amount of SiC in the C50 composition, irregular SiC grains no longer stood out in the microstructure, with many of them coated by the phases resulting from the infiltration. As the amount of kaolin in the composition increased, the SiC grains became increasingly less visible until the finest particles, products of the infiltration, completely coated the SiC grains. A comparison of this composition against the C10 one reveals mainly greater quantities of silicon, aluminum, and alumina in the microstructure. Since this composition contains a much larger quantity of kaolin and quartz, according to reaction 1, a greater precipitation of alumina and, hence, of silicon in the microstructure is expected, as indicated in the micrograph and confirmed by the diffractogram in Fig. 5. Metallic silicon also appears around the few visible SiC grains and is also associated with metallic aluminum. The XRD diffractogram clearly shows the larger quantity of aluminum, followed by silicon and oxygen. Comparing this image with that of the C10 composite, it is clear that the larger quantity of aluminum and oxygen is associated with the formation of alumina in the microstructure, as indicated in the XRD diffractograms.

Properties of mechanical strength and hardness of the composites

Table 3 lists the results of the measurements of flexural strength and microhardness of the composites.

In comparison with the SiC 200 system, note the increase in mechanical strength of the composite, which is associated with the increase in the kaolin concentration in the compositions, up to C40. The addition of only 10% of kaolin propelled the mechanical strength up from 160 MPa (pure SiC) to 240 MPa, representing an increase of approximately 51%. The other composites, namely C20C, C30C, and C40C, showed increases to 100, 135, and 140 MPa, translating into percentile increases of 62.5, 84.4, and 87.5%, respectively. However, the C50 composite

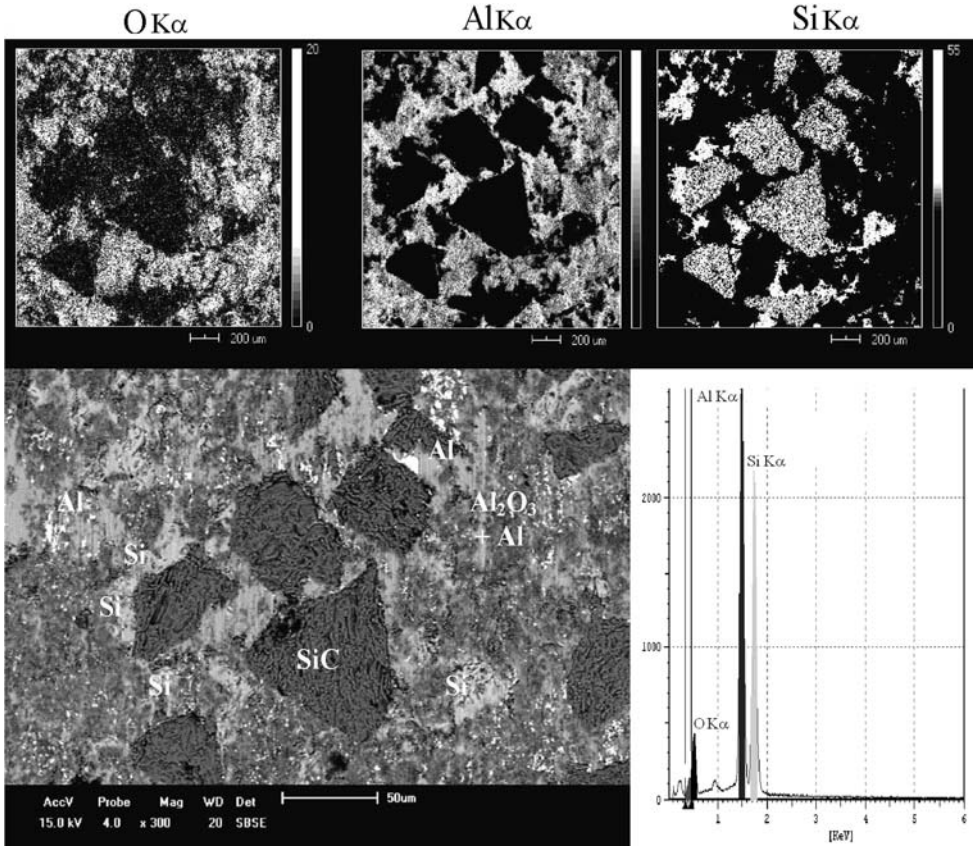

Fig. 7 EDX microstructural mapping of the chemical elements of composite C10C

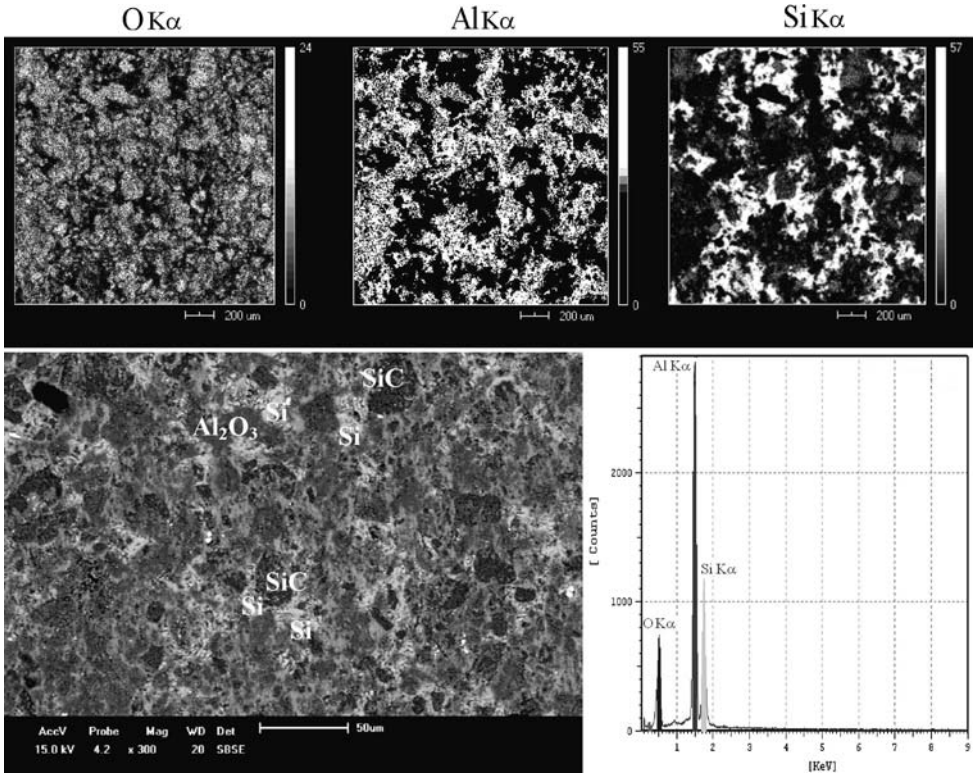

Fig. 8 EDX microstructural mapping of the chemical elements of composite C50C

Table 3 Properties of mechanical strength and microhardness of the composites

Composition	Flexural strength (MPa)	Vickers microhardness (kgf/mm^2)
SiC 200	160	180
C10	240	234
C20	260	247
C30	295	346
C40	300	333
C50	280	380

showed a 20 MPa reduction in mechanical strength compared with that of composite C40C, indicating a tendency for the mechanical properties to decline at kaolin concentrations exceeding 40%. In view of these findings, we conclude that 40% of kaolin is the optimized amount. Compositions with high mechanical strength and minimized quantities of SiC are highly favorable for these composites, particularly considering their cost, since SiC is a costly synthetic product. Another positive factor is that the deleterious Al_4C_3 phase commonly found in infiltrations of SiC–Al were not characterized in these composites.

In the preparation of the preform at 1100 °C, kaolinite transforms into mullite, releasing SiO_2, which is added to the SiO_2 present in kaolin as an impurity. These phases are reduced during infiltration by reaction with the molten metallic aluminum, producing the precipitation of alumina in the microstructure. As the quantity of kaolin in the composition increases, larger amounts of alumina are precipitated, contributing to increase the mechanical strength of the composite. Starting from C10, with the increase in the amount of alumina in the microstructure, this begins to govern the mechanical strength and the SiC particles begin to act as reinforcements. The reduction in mechanical strength of the C50 composition, even with the increased precipitation of alumina in the microstructure, is probably associated with the smaller amount of SiC phase reinforcing the matrix, thus reducing the crack propagation pathway and diminishing the composite's mechanical strength. This behavior is according with other study, where was concluded that the improvement of fracture toughness is directly related to the bimodal microstructure with large grains in the fine matrix grains, which arose from the residual stress, grain pullout, crack bridging, and crack deflection [22].

Generally speaking, hardness is directly related with the amount of kaolin added to the matrix, i.e., the larger the quantity of kaolin the higher the hardness, up to the limit of 40% of kaolin. Depending on the concentration of kaolin in the preform, the mechanical strength of the composites obtained in this work varied from 160 to 300 MPa, presenting intermediary values when compared with other studies of aluminum-infiltrated SiC-based composites, whose values varied from 70 to 558 MPa [4, 8, 9, 12, 14, 15]. On the other hand, higher values of hardness were obtained in this work, reaching up to 472 kgf/cm^2, which is far superior to that of other composites reported in the literature [14]. These higher hardness values are likely attributable to the higher concentration of alumina in the microstructure, originating from the reaction between liquid aluminum and the mullite and quartz phases in the perform. However, a Vickers hardness of 620 kgf/cm^2 was measured in an aluminum-infiltrated silica glass matrix [10], which is much higher than that obtained in this work, and was attributed to the presence of alumina in the composite's microstructure. In other words, high hardness values are associated with a higher concentration of alumina in the microstructure of the composite.

Conclusions

Depending on the composition, SiC–kaolin–Al composites can be used in applications that require high flexural strength (240–300 MPa), low density, and surface hardness of 180–380 kgf/mm^2. Molten aluminum reacted preferentially with quartz and other aluminosilicates in the preform, reducing them and precipitating alumina and silica in the microstructure. The preforms also contained excess aluminum that did not react in the process. This preferential reaction with the silicates of the preform prevented the reaction of aluminum with SiC, precluding the formation of Al_4C_3 phase, which is highly hygroscopic and causes degradation of the composite. Increasing amounts of kaolin led to increasing mechanical strength and hardness of the composite, a behavior that was attributed to the higher concentration of alumina in the microstructure. At concentrations of more than 40% kaolin, a slight decline in mechanical strength was observed due to the decreased concentration of SiC particles, which act as matrix reinforcement. An additional advantage is the composite's cost, since kaolin is an inexpensive raw material that supplies silica and alumina, and can be used in concentrations of up to 40% to substitute SiC in the composition, improving the final properties in comparison with pure SiC–Al.

Acknowledgements We are pleased to acknowledge the financial support for this research by the National Counsel of Technological and Scientific Development (CNPq) and Coordination for the Improvement of the Higher Level Personnel (CAPES), Brazil.

References

1. Chawla KK (1987) Composite materials, science and engineering. Springer-Verlag, New York
2. Nascimento RM, Martinelli AE, Buschinelli AJA (2003) Cerâmica 49:178

3. Ohnabe H, Masaki S, Onozuka M et al (1999) Composites Part A 30:489
4. Pech-Canul MI, Makhouf M (2000) J Mater Synth Process 8:35
5. Garcia-Cordovilla C, Louis E, Narciso J (1999) Acta Mater 47:4461
6. Yue HY, Fei WD, Wang LD (2008) J Mater Sci 43:6233. doi:10.1007/s10853-008-2914-5
7. Zhang Z, Chen XG, Charette A (2009) J Mater Sci 44:492. doi:10.1007/s10853-008-3097-9
8. Demir A, Altinkok N (2004) Compos Sci Technol 64:2067
9. Zhu Y, Huang Z, Dong S et al (2007) J Am Ceram Soc 90:969
10. Lee JC, Ahn JP, Shim JH et al (1999) Scripta Mater 41:895
11. Rodrígues-Reyes M, Pech-Canul MI, Redón-Angeles JC et al (2006) Compos Sci Technol 66:1056
12. Altinkok N (2004) J Compos Mater 38:1533
13. Hwu BK, Lin SJ, Jahn MT (1996) Mater Sci Eng A 207:135
14. Ahlatci H, Candan E, Çimenoglu H (2004) Metall Mater Trans A 35A:2127
15. Thünemann M, Beffort O, Kleiner S et al (2007) Compos Sci Technol 67:2377
16. Scudino S, Surredi KB, Sager S, Sakaliyska M, Kim JS, Loser W, Echert J (2008) J Mater Sci 43:4518. doi:10.1007/s10853-008-2647-5
17. Santos PS (1989) Ciência e Tecnologia de Argilas. Edgar Blucher, São Paulo
18. Liu W, Koster U (1996) Mater Sci Eng A 210:1
19. Pech-Canul MI, Katz RN, Makhlouf MM, Pickard S (2000) J Mater Sci 35:2167. doi:10.1023/A:1004758305801
20. Mirbagheri SMH, Sookhtehsaraee S (2008) J Mater Sci 43:6944. doi:10.1007/s10853-008-2973-7
21. Fahrenholtz WG, Ewsuk KG, Loehman RE (1998) J Am Ceram Soc 81:2533
22. Wang B, Yang J, Guo R, Gao J, Yang J (2009) J Mater Sci 44:1351. doi:10.1007/s10853-008-3009-z